*Bm*K CT enhances the sensitivity of temozolomide-induced apoptosis of malignant glioma U251 cells *in vitro* through blocking the AKT signaling pathway

JUN DU[1*], RUIJIE WANG[1*], LITIAN YIN[2], YUEJUN FU[1], YUQING CAI[1], ZHIYUN ZHANG[1] and AIHUA LIANG[1]

[1]Key Laboratory of Chemical Biology and Molecular Engineering of Ministry of Education, Institute of Biotechnology, Shanxi University; [2]Department of Physiology, Key Laboratory of Cellular Physiology Co-Constructed by Province and Ministry of Education, Shanxi Medical University, Taiyuan, Shanxi 030006, P.R. China

Received May 9, 2017; Accepted November 9, 2017

DOI: 10.3892/ol.2017.7483

Abstract. Temozolomide (TMZ) is a drug that has been demonstrated to improve the survival time of patients with glioblastoma multiforme (GBM) when administered with concomitant radiotherapy. However, chemoresistance is one of the major obstacles in the treatment of GBM. In the present study, an MTT assay and flow cytometry were used to demonstrate that chlorotoxin-like toxin in the venom of the scorpion *Buthus martensii* Kirsch (*Bm*K CT) markedly inhibited cell proliferation and induced apoptosis in U251 cells when combined with TMZ. In combination with TMZ, *Bm*K CT exhibited a significant and synergistic anti-tumor effect by inhibiting protein kinase B (AKT) independently and triggering the apoptosis signaling cascade *in vitro*. Furthermore, *Bm*K CT increased the expression of phosphatase and tensin homolog at the transcriptional level, which is a key negative regulator of the AKT signaling pathway. The results of the present study demonstrated that *Bm*K CT enhanced the sensitivity of TMZ-induced U251 cell apoptosis through the downregulation of phosphorylated AKT levels, suggesting that *Bm*K CT and TMZ combination therapy may be a novel approach for glioma therapy.

Introduction

Glioma is a common type of primary brain tumor, making up ~30% of all brain and central nervous system tumors and 80% of all malignant brain tumors (1,2). Therapy for the treatment of gliomas consists of tumor resection, followed by radiotherapy and chemotherapy that usually involves O^6-alkylating agents (3-5). Despite improvements in the standard of care, the median overall survival (OS) time for patients with glioblastoma multiforme (GBM) has only marginally improved over the past decade, and remains approximately one year (3,4). Thus, therapeutic approaches to cure this malignancy are urgently required to advance treatment.

Temozolomide (TMZ), an alkylating agent with simple oral administration, is used in combination with and following radiotherapy (5,6). Due to the overexpression of phosphorylated protein kinase B (p-AKT), an increasing number of TMZ-resistant cases have been reported clinically (7). AKT is a major downstream target of growth factor receptor tyrosine kinases that signal via phosphoinositide 3-kinase (PI3K) (8,9). Activation of AKT has been demonstrated to be associated with increased tumorigenicity and invasiveness (10). Inhibitors of the PI3K/AKT signaling pathway, including NVP-BEZ235 and GDC-0941, have been identified to enhance the cytotoxicity of TMZ (7,11,12).

The excessive growth and metastasis of malignant gliomas may be controlled by a recombinant chlorotoxin-like toxin in the venom of the scorpion *Buthus martensii* Kirsch (*Bm*K CT) fusion protein (13). Similarly, the significance of *Bm*K CT had been well documented as a novel blocker of chloride channels and matrix metallopeptidase 2 (14,15). Based on the aforementioned preclinical studies, the combination of *Bm*K CT and TMZ may be an effective treatment for patients with GBM. Therefore, *Bm*K CT combined with TMZ in glioma treatment was deemed to be worthy of further study.

In the present study, the antitumor effect of glutathione S-transferase (GST)-*Bm*K CT combined with TMZ was investigated using the human malignant glioma U251 cell line. The molecular mechanisms underlying this synergistic effect were also investigated.

Materials and methods

Materials and protein preparation. The gene sequence of *Bm*K CT was amplified by polymerase chain reaction (PCR)

Correspondence to: Professor Aihua Liang, Key Laboratory of Chemical Biology and Molecular Engineering of Ministry of Education, Institute of Biotechnology, Shanxi University, 92 Wucheng Road, Taiyuan, Shanxi 030006, P.R. China
E-mail: aliang@sxu.edu.cn

*Contributed equally

Key words: glioma, *Buthus martensii* Kirsch, chlorotoxin-like toxin, temozolomide, apoptosis, protein kinase B, signaling pathway

from the vector pRSETc-*Bm*K CT (constructed in Molecular Biology Laboratory, Institute of Biotechnology, Shanxi University, Taiyuan, China) and cloned into pGEX-6p-1 (GE Healthcare Life Sciences, Shanghai, China) to construct the expression vector. The forward primer was 5'-CGCGGATCC ATGTGCGGTCCGTGCTTC-3' (*Bam*HI enzyme site), and the reverse primer was 5'-CCGCTCGAGTCAGATACGGTT GCACAG-3' (*Xho*I enzyme site). PCR was performed using Taq DNA polymerase (cat no. RR001A; Takara Biotechnology Co., Ltd., Dalian, China) and the thermocycling conditions were as follows: 95˚C for 5 min, 40 cycles at 95˚C for 30 sec, 63˚C for 30 sec and 72˚C for 30 sec, followed by 72˚C for 5 min. The product of the PCR was fused with the GST gene under the regulation of the tac promoter (Ptac). The expression of Ptac was proportional to the concentration of isopropyl β-D-1-thiogalactopyranoside (IPTG). The recombinant plasmid pGEX-6p-1-*Bm*K CT was transformed into *E. coli* BL21 (DE3). The recombinant GST-*Bm*K CT fusion protein was induced using 0.4 mM IPTG at 37˚C for 4 h and purified using a GSH affinity chromatography column (GE Healthcare Life Sciences) according to manufacturer's protocols. Minipreparation of GST protein was performed and the protein was purified using a GSH affinity chromatography column via the transformation of empty plasmid pGEX-6p-1 into *E. coli* BL21 (DE3), and was then used as a control sample in the present study. The expression and purification of GST and GST-*Bm*K CT proteins were analyzed using 10% SDS-PAGE gel. The U251 human GBM cell line was kindly provided by Dr Tao Hu (Department of Neurosurgery, Shanxi Provincial People's Hospital, Taiyuan, China).

Cell culture. Cell cultures were prepared and maintained according to standard cell culture procedures. The human glioma cell line U251 was cultured in complete medium, consisting of Dulbecco's modified Eagle's medium (Gibco; Thermo Fisher Scientific, Inc., Waltham, MA, USA) containing high glucose and pyruvate, supplemented with 10% fetal bovine serum (FBS Premium; PAN-Biotech GmbH, Aidenbach, Germany), 2 mM glutamine, 100 U ml^{-1} penicillin G and 100 ng ml^{-1} streptomycin. Cells were maintained at 37˚C in a humidified 5% CO_2 atmosphere. The cells were dissociated using TE (0.25% trypsin and 0.02% EDTA solution; Gibco; Thermo Fisher Scientific, Inc.). For the apoptotic experiments, cells were dissociated using 0.25% Trypsin and EDTA free solution (Gibco; Thermo Fisher Scientific, Inc.).

Drug treatment. Cells were harvested and $5x10^4$ cells were plated in each well of 12-well plate and after 24 h later, cells were treated with 1.12 μM GST, 1.12 μM GST-*Bm*K CT and 0.1 mM TMZ (Merck & Co., Inc., Whitehouse Station, NJ, USA). *Bm*K CT was a homolog of chlorotoxin (CTX). CTX could inhibit U251 cell transwell migration at the inhibition rate of 56.26% under 1 μM (16). Based on the aforementioned study, the concentration of *Bm*K CT used in the present study was set at 1.12 μM. The half maximal inhibitory concentration (IC_{50}) value of TMZ, defined as the concentration that reduces the global growth of cells by 50%, was previously determined to be ~0.2 mM (17). Therefore, the concentration of TMZ used in the present study was set at 0.1 mM, which was the same as published data of TMZ used for glioma cells (17,18). TMZ stocks were prepared by dissolving the drug in dimethyl sulfoxide and stored at 4˚C. Following treatment, cells were gently washed with phosphate buffer saline (PBS), incubated in fresh media at 37˚C, and harvested at various time periods.

Cell viability assay. Cell viability was assessed using the MTT method. A total of $1x10^3$ cells were seeded into each well of a 96-well culture plate. In brief, U251 cells were treated with GST, GST-*Bm*K CT and TMZ, and incubated for 1, 2, 3, 4 and 5 days. The liquid was discarded and 100 μl sanlian dissolved liquid (10% SDS, 5% isobutyl alcohol, 0.01 M HCl) was added to dissolve the purple formazan. The absorbance at 570 nm was measured using a microplate reader following incubation. Subsequently, a calibration curve was prepared using the data obtained from the wells that contained known numbers of viable cells. The experiment was performed in six replicates and repeated three times.

Cell cycle assay. U251 cells were plated at a density of $5x10^4$ cells per well in 12-well plates. After 96 h of treatment with GST or GST-BmK CT in the presence or absence of TMZ, cells were harvested and fixed in 70% ethanol at -20˚C overnight. Subsequently, the cells were washed and resuspended in 100 μl PBS containing 5 μg/ml propidium iodide (PI; Sigma-Aldrich; Merck KGaA, Darmstadt, Germany) and 100 μg/ml RNase A (Fermentas; Thermo Fisher Scientific, Inc.) for 1 h at room temperature in the dark. Each group of $2x10^4$ cells were subsequently analyzed using a FACSCalibur flow cytometer (BD Biosciences, Franklin Lakes, NJ, USA); data were analyzed using FlowJo software (version 7.6; FlowJo LLC, Ashland, OR, USA). Cell cycle status was determined by measuring the cellular DNA content, following staining with PI.

Apoptosis assay. A total of $5x10^4$ U251 cells were plated onto 12-well plates and treated with GST-*Bm*K CT (1.12 μM), TMZ (100 μM), and the combination of the two, respectively. The apoptosis ratio was analyzed 96 h post-treatment using a StarGlow Annexin V-fluorescein isothiocyanate (FITC)/PI Apoptosis Detection kit (cat no. c203-05; GenStar BioSolutions Co., Ltd., Beijing, China). Annexin V-FITC and PI double staining was performed at room temperature for 5 min and was used to evaluate the percentage of apoptotic cells. Annexin V^- and PI^- cells were used as the controls. Annexin V^+ and PI^- cells were designated as those in early-stage apoptosis, Annexin V^- and PI^+ cells were designated as necrotic, and Annexin V^+ and PI^+ cells as late-stage apoptosis. The stained cells were quantified using a FACSCalibur flow cytometer (BD Biosciences) and analyzed using FlowJo software. Tests were replicated in triplicate, and repeated three times.

RNA isolation and reverse transcription-quantitative (RT-q) PCR. Total mRNA was isolated from tumor cells using TRIzol™ Reagent (Invitrogen; Thermo Fisher Scientific, Inc.), according to the manufacturer's protocol. cDNA was synthesized using the PrimeScript® First Strand cDNA Synthesis kit (cat no. D6110A; Takara Biotechnology Co., Ltd., Dalian, China). The transcription conditions were as follows: 37˚C for 15 min, 85˚C for 5 sec and 4˚C for 5 min. qPCR was performed using the CFX96 Real-Time PCR Detection System (cat

no. 185-5195; Bio-Rad Laboratories, Inc., Hercules, CA, USA) with the SYBR® PrimeScript™ RT-PCR kit (cat no. DDR083A; Takara Biotechnology Co., Ltd.). The thermocycling conditions were as follows: 95˚C for 5 min, followed by 40 cycles at 95˚C for 5 sec and 60˚C for 30 sec. The $2^{-\Delta\Delta Cq}$ method was used to quantify gene expression (19). Transcript levels were normalized to those of GAPDH. The primers sequences for RT-qPCR were as follows: PTEN forward, 5'-CCTTCT CCATCTCCTGTGTAATCAA-3' and reverse, 5'-GTTGAC TGATGTAGGTACTAACAGCAT-3'; and GAPDH forward, 5'-AACGGGAAGCTTGTCATCAATGGAAA-3' and reverse, 5'-GCATCAGCAGAGGGGGCAGAG-3'.

Western blot analysis. U251 cells were treated with GST, GST-*Bm*K CT or TMZ for 1, 2, 4, 8 and 16 h. Subsequently, the cultured cells were washed twice in PBS after treatment at the indicated time points (0, 1, 2, 4, 8 and 16 h) prior to lysis using the M-PER® Mammalian Protein Extraction Reagent (cat no. 75801; Thermo Fisher Scientific, Inc.) supplemented with a proteinase inhibitor cocktail (cat no. 04693116001; Roche Diagnostics GmbH, Mannheim, Germany), phosphatase inhibitor cocktail (cat no. 04906845001; Roche Diagnostics GmbH) and phenylmethylsulfonyl for 30 min on ice. The concentration of protein was quantitated using a BSA kit (cat no. QJ223202; Thermo Fisher Scientific, Inc.). An equal amount (20 μg/lane) of protein lysates was resolved to 10% SDS-PAGE gel. Proteins were transferred onto polyvinylidene difluoride membranes with a 0.45 μm pore size (EMD Millipore, Billerica, MA, USA), which were then blocked with 5% bovine serum albumin at room temperature for 1 h and probed with primary antibodies at 4˚C overnight. The following primary antibodies, all of which were diluted at 1:1,000, were used in the present study: Anti-GST (cat no. D110271; Sangon Biotech), anti-β-actin (cat no. LK9001L; Tianjin SunGene Biotech Co., Ltd., Tianjin, China), anti-AKT (cat no. 2920S; Cell Signaling Technology, Inc., Danvers, MA, USA), anti-p-AKT (cat no. 4060S; Cell Signaling Technology, Inc.), anti-B cell lymphoma 2 (Bcl-2; cat no. 3498S; Cell Signaling Technology, Inc.), anti-Bcl-2 associated X protein (Bax; cat no. 2772S; Cell Signaling Technology, Inc.), anti-caspase-9 (cat no. ab202068; Abcam, Cambridge, UK) and anti-caspase-3 (cat no. 9664S; Cell Signaling Technology, Inc.). They were subsequently incubated with a secondary horseradish peroxidase-conjugated goat anti-rabbit IgG antibody (cat no. 31210; dilution, 1:5,000) or a goat anti-mouse IgG antibody (cat no. 31431; dilution, 1:5,000; both Thermo Fisher Scientific, Inc.) at room temperature for 1 h. Results were visualized using the SuperSignal West Dura chemiluminescent substrate (cat no. QJ220977; Thermo Fisher Scientific, Inc.). ImageJ software (National Institutes of Health, Bethesda, MD, USA) was used to quantify the band density.

Statistical analysis. Data are presented as the mean ± standard deviation. Experiments were repeated three or six times. Statistical analyses were performed using GraphPad Prism 5.0 (GraphPad Software, Inc., La Jolla, CA, USA). Two-way analysis of variance, followed by a Bonferroni's post hoc test, and the Student's t-test were applied to calculate the statistical difference as appropriate. P<0.05 was considered to indicate a statistically significant difference.

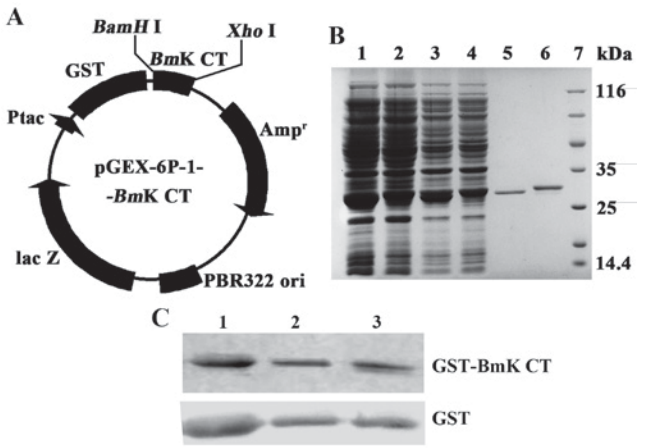

Figure 1. Construction of pGEX-6P-1-*Bm*K CT and production of recombinant GST-*Bm*K CT. (A) The *Bm*K CT gene was cloned into pGEX-6p-1 to construct the expression vector pGEX-6P-1-*Bm*K CT. (B) SDS-PAGE analysis of the expression and purification of GST and GST-*Bm*K CT. Lane 1-2: The total expressed proteins of BL21(DE3)/pGEX-6P-1 or BL21(DE3)/pGEX-6P-1-*Bm*K CT induced by 0.4 mM IPTG for 4 h; lane 3-4: The proteins after binding to glutathione sepharose beads; lane 5-6: Purified GST or GST-*Bm*K CT extracted by GSH affinity chromatography; lane 7: molecular mass markers. (C) Western blotting was used to identify GST-*Bm*K CT or GST among the total expressed proteins (lane 1), the proteins after binding to glutathione sepharose beads (lane 2), and the purified proteins (lane 3). GST-*Bm*K CT, Glutathione S-transferase fused with *Buthus martensii* Kirsch chlorotoxin-like toxin.

Results

Construction and purification of recombinant GST-BmK CT. The gene *Bm*K CT was fused with GST via the *Bam*HI and *Xho*I sites under the regulation of Ptac (Fig. 1A). The pGEX-6p-1-*Bm*K CT was transfected into *E. coli* BL21 (DE3). Then the recombinant protein GST-*Bm*K CT was expressed via induction with IPTG. The recombinant protein was collected and concentrated into PBS. A BCA kit was used to determine the concentration of protein. The GST-*Bm*K CT protein concentration was 6.62 mg/ml (224 μM). GST was produced via the same strategy and the concentration was adjusted to 224 μM. The proteins were diluted to 1.12 μM in complete medium. The expressed proteins of BL21 (DE3)/pGEX-6P-1 or BL21(DE3)/pGEX-6P-1-*Bm*K CT, the proteins bound to glutathione sepharose beads, and purified GST or GST-*Bm*K CT were analyzed using 10% SDS-PAGE gel (Fig. 1B) and immunologically identified using western blot analysis (Fig. 1C).

GST-BmK CT increases the inhibitive effect of TMZ on U251 cell viability. The number of GST and GST-*Bm*K CT-treated cells following TMZ administration were detected using an MTT assay at 1, 2, 3, 4 and 5 days post treatment. In this assay, GST protein demonstrated no effect on the proliferation of U251 cells, as compared with the control group. However, GST-*Bm*K CT protein and TMZ inhibited the growth of U251 cells in a time-dependent manner, compared with the control group (P<0.001). Furthermore, there was an increased inhibitory effect when GST-*Bm*K CT was combined with TMZ

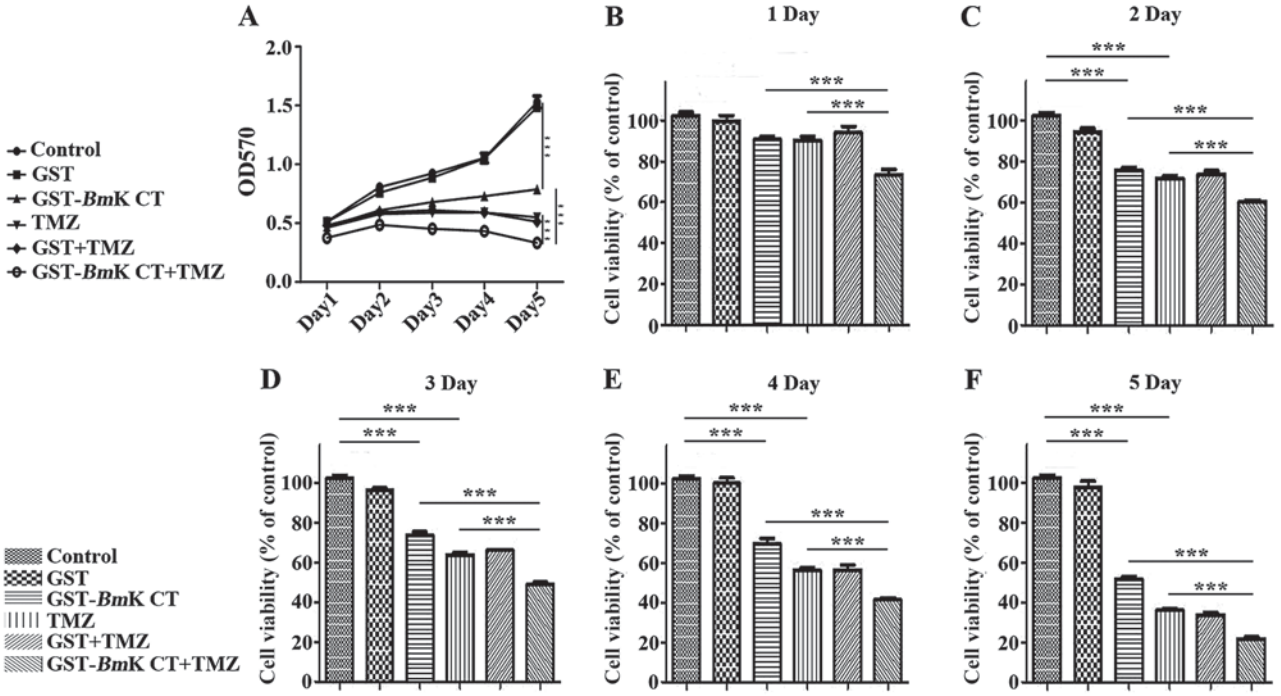

Figure 2. Effect of GST-*Bm*K CT combined with TMZ on the proliferation of U251 cells. (A) MTT analysis was performed at (B) 1, (C) 2, (D) 3, (E) 4 and (F) 5 days after treatment. Data are presented as the mean ± standard deviation of six replicates. ***P<0.001. GST-*Bm*K CT, *Buthus martensii* Kirsch; TMZ, temozolomide.

compared with the effects of individual treatments (P<0.001) (Fig. 2A-F). The MTT assay revealed that TMZ treatment decreased cell viability to 36±1.8% of the control. When TMZ was combined with *Bm*K CT, cell viability was further inhibited to 22±2.0% of the control after 5 days (Fig. 2F). These results demonstrated that TMZ combined with *Bm*K CT inhibited the viability of U251 cells by an increased degree (Fig. 2), compared with TMZ single treatment, decreasing the IC_{50} value from a previously reported 0.2 mM (17) to 0.1 mM. This suggested that GST-*Bm*K CT protein and TMZ synergistically (20) inhibit U251 glioma cell growth.

GST-BmK CT enhances TMZ-induced cell cycle arrest in U251 cells. To study the anti-proliferative mechanism of *Bm*K CT combined with TMZ, the effect of this combination treatment on the glioma cell cycle was investigated. U251 cells were cultured with 1.12 μM GST or GST-*Bm*K CT in the presence or absence of 100 μM TMZ for 96 h, following which the cell cycle status was analyzed using flow cytometry. As presented in Fig. 3, *Bm*K CT treatment resulted in cell cycle arrest in the S phase, an effect which did not occur in the control and GST treatment groups. Treatment with TMZ induced G_2/M phase arrest. Notably, markedly prolonged S and G_2/M phase arrest durations were observed when *Bm*K CT and TMZ were used in combination (Fig. 3).

GST-BmK CT improves TMZ-induced U251 cell apoptosis. To assess the pro-apoptotic effect of *Bm*K CT combined with TMZ, U251 cells were treated with *Bm*K CT in the presence or absence of TMZ. Apoptotic cells were measured using an Annexin-V/PI staining assay. As presented in Fig. 4A, U251 cells treated with GST-*Bm*K CT protein or TMZ exhibited an increased rate of apoptosis, compared with the control. In particular, there was a significant increase in the number of apoptotic cells in the combined GST-*Bm*K CT and TMZ treatment group (Fig. 4B). By analyzing the proportions of early- and late-apoptotic cells, GST-*Bm*K CT protein combined with TMZ were identified to have an increased effect on the number of early-apoptotic cells compared with TMZ alone, which was increased by ~2.5-fold (Fig. 4C and D).

GST-BmK CT protein induces U251 cell apoptosis by downregulating p-AKT. AKT phosphorylation triggers resistance to TMZ and upregulates the expression of various anti-apoptosis-associated proteins (7). To understand the mechanisms underlying the apoptosis induced by the combined treatment, the levels of AKT phosphorylation and apoptosis-associated proteins were investigated using western blot analysis. The results demonstrated that in GST-*Bm*K CT treated U251 cells for 16 h, the phosphorylation of AKT was significantly decreased compared with the control (0 h; Fig. 5A; P<0.005), while the phosphorylation of AKT in GST-treated or TMZ-treated U251 cells did not change (Fig. 5B and C). In addition, the levels of Bax (Fig. 5D), cleaved caspase-3 and cleaved caspase-9 (Fig. 5E) were increased in GST-*Bm*K CT treated U251 cells compared with the control (0 h). The expression level of Bcl-2 was revealed to be decreased in the *Bm*K CT treatment group (Fig. 5D). Furthermore, GST-*Bm*K CT increased the transcription of phosphatase and tensin homolog (PTEN), which is a major negative regulator of the AKT signaling pathway (21) (Fig. 5F); however TMZ did not perform the same function (Fig. 5G).

GST-BmK CT synergistically enhances the apoptosis-inducing effects of TMZ in U251 cells via the downregulation of p-AKT.

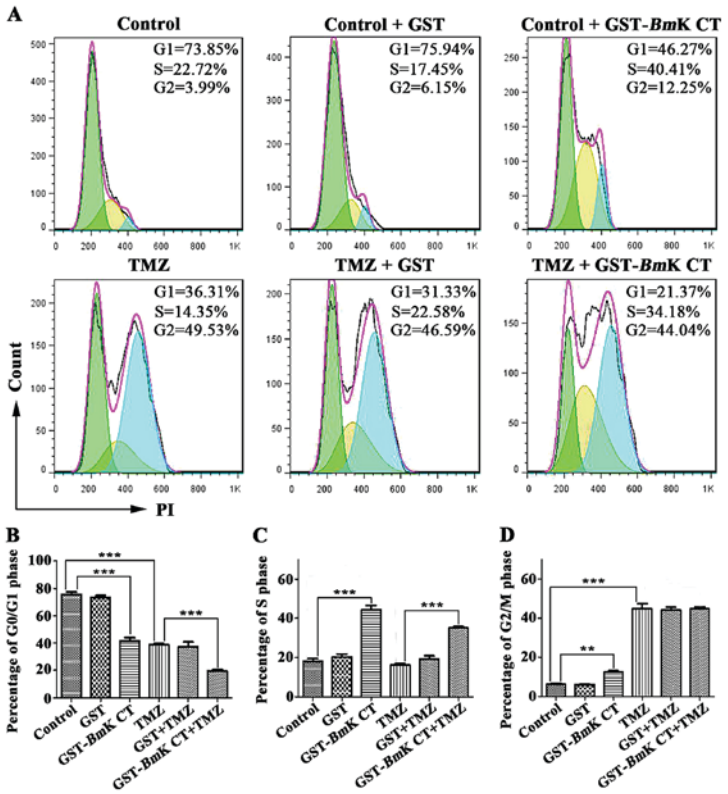

Figure 3. Cell cycle arrest in U251 cells treated with GST-*Bm*K CT, TMZ, and the combination treatment. (A) Representative results of the percentage of cells in the G_0/G_1, S, or G_2/M phases among U251 cells exposed to GST, GST-*Bm*K CT, TMZ or their combination for 96 h, as detected by flow cytometry. The total number of cells per group exposed to flow cytometry was 20,000. Histograms indicate the percentage of U251 cells in the (B) G_0/G_1, (C) S, and (D) G_2/M phases in three independent experiments. The data are presented as the average of triplicate results from a representative experiment. Bars represent the standard deviation. **P<0.005, ***P<0.001. GST-*Bm*K CT, Glutathione S-transferase fused with *Buthus martensii* Kirsch chlorotoxin-like toxin; TMZ, temozolomide; PI, propidium iodide.

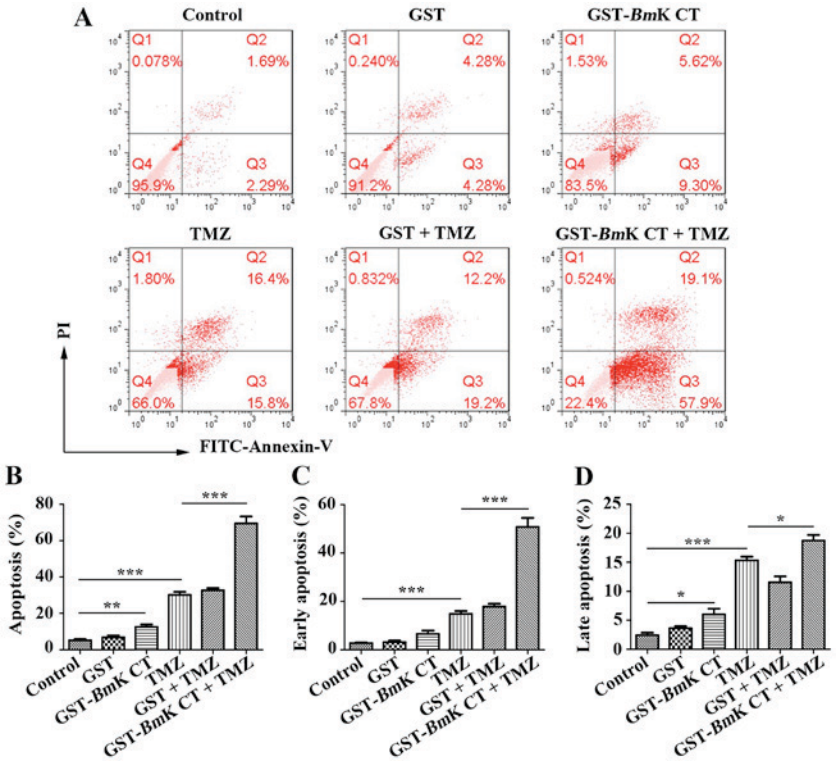

Figure 4. GST-*Bm*K CT combined with TMZ enhanced the apoptosis rate of U251 cells. (A) The number of apoptotic cells was determined via flow cytometry 4 days after treatment. (B) The total, (C) early- and (D) late-apoptotic cell numbers were analyzed. Data are presented as the mean ± standard deviation of three replicates. Apoptosis experiments were repeated ≥3 times. *P<0.05, **P<0.005, ***P<0.001. GST-*Bm*K CT, Glutathione S-transferase fused with *Buthus martensii* Kirsch chlorotoxin-like toxin; TMZ, temozolomide; PI, propidium iodide; FITC, fluorescein isothiocyanate.

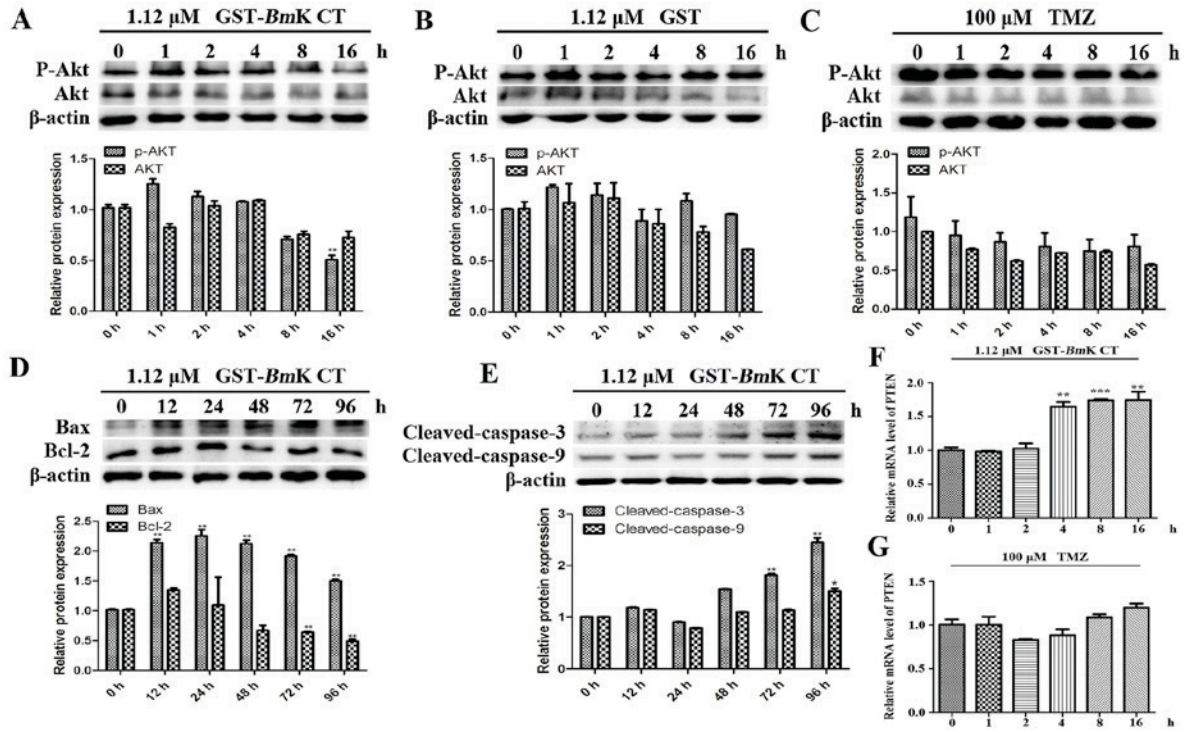

Figure 5. *Bm*K CT induced U251 cell apoptosis through downregulating p-AKT. AKT and p-AKT levels were measured in U251 cells treated with (A) 1.12 μM GST-*Bm*K CT, (B) 1.12 μM GST or (C) 100 μM TMZ for 0, 1, 2, 4, 8 or 16 h, using western blotting and the densitometric quantification of AKT and p-AKT was normalized to β-actin. (D) Western blot analysis of Bcl-2, Bax and (E) caspase-3/9 levels and the quantification was normalized to β-actin in the U251 cells stimulated with GST-*Bm*K CT (1.12 μM) for 0, 12, 24, 48, 72 or 96 h. For caspase-3/-9, the antibody was directed against the active fragment. The relative mRNA expression levels of PTEN were assayed by quantitative polymerase chain reaction following the treatment of U251 cells with (F) 1.12 μM GST-*Bm*K CT or (G) 100 μM TMZ for 0, 1, 2, 4, 8 or 16 h. Data are presented as the mean ± standard deviation of three replicates. *P<0.05, **P<0.005, ***P<0.001 vs. untreated cells. GST-*Bm*K CT, Glutathione S-transferase fused with *Buthus martensii* Kirsch chlorotoxin-like toxin; TMZ, temozolomide; Bcl-2, B cell lymphoma 2; Bax, Bcl-2 associated X protein; PTEN, phosphatase and tensin homolog; ns, not significant; AKT, protein kinase B.

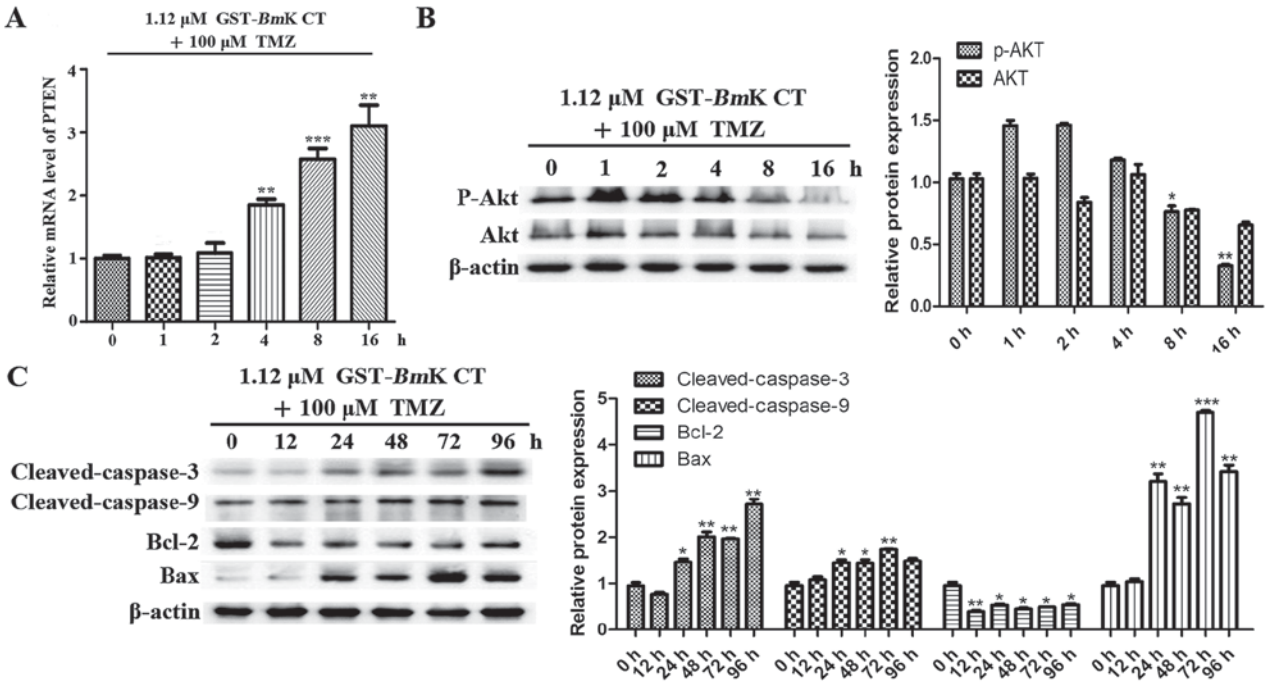

Figure 6. *Bm*K CT enhanced the TMZ-sensitivity and the apoptotic response of U251 cells by downregulating AKT phosphorylation. (A) The relative mRNA expression levels of PTEN were investigated using quantitative polymerase chain reaction following the combination treatment of U251 cells with 1.12 μM GST-*Bm*K CT and 100 μM TMZ in a time-dependent manner. (B) Western blot analysis was performed to evaluate the levels of p-AKT, AKT and (C) various apoptotic proteins in *Bm*K CT and TMZ combination-treated U251 cells. The bands were quantified respectively. Data are presented as the mean ± standard deviation of three replicates. *P<0.05, **P<0.005, ***P<0.001 vs. untreated cells. GST-*Bm*K CT, Glutathione S-transferase fused with *Buthus martensii* Kirsch chlorotoxin-like toxin; TMZ, temozolomide; Bcl-2, B cell lymphoma 2; Bax, Bcl-2 associated X protein; PTEN, phosphatase and tensin homolog; ns, not significant; AKT, protein kinase B.

To investigate the contribution of *Bm*K CT to the effects of TMZ, parallel studies were performed, in which U251 cells were treated with *Bm*K CT and TMZ for different lengths of time. As presented in Fig. 6A, the transcription PTEN was increased compared with the control (0 h) when the cells were stimulated by GST-*Bm*K CT protein combined with TMZ. The results revealed that this drug combination may enhance the suppressive effect on AKT phosphorylation (Fig. 6B) and the upregulation of pro-apoptotic proteins in U251 cells (Fig. 6C), compared with the control (0 h). Taken together, these results suggest that *Bm*K CT enhances the apoptosis sensitivity of TMZ-treated U251 glioma cells by downregulating p-AKT.

Discussion

Accumulating evidence has demonstrated that GBM is resistant to TMZ (7,11,12,22,23). A possible reason for this is that GBM may affect AKT activity and protect against drug-induced cytotoxicity (22,23). In addition, clinical evidence has identified that primary or acquired resistance to TMZ is a major therapeutic problem (11). Therefore, a combination therapy that enhances the efficacy of TMZ is required.

*Bm*K CT is a short chain peptide consisting of 35 amino acid residues with four disulfide bridges, and specifically targets glioma cells and inhibits glioma cell growth without any notable toxicity to normal astrocytes (13). In the present study, the synergistic effect and mechanism of *Bm*K CT involved in enhancing cell sensitivity to TMZ-induced apoptosis was investigated using malignant glioma U251 cells. The absence of structural characterization of recombinant GST-BmK CT, which contains a 36-mer peptide, is a limitation of the present study.

The results of the present study demonstrated that *Bm*K CT enhances the sensitivity of malignant glioma U251 cells to TMZ-induced apoptosis via the AKT signaling pathway; inhibiting the growth, invasion and migration of glioma cells. It was identified that *Bm*K CT alone induced S phase arrest; however, when combined with TMZ, the treatment significantly induced G_2/M arrest and cell death. These data revealed that *Bm*K CT arrested the cell cycle at the G_2/M phase following TMZ-induced DNA damage, in addition to blocking effects at the S/G_2 transition. Although it is a protein oligopeptide that has been extensively studied, whether it may be an agent with improved ability to cause glioma cell apoptosis when combined with TMZ requires further study. In the present study, the MTT, apoptosis and flow cytometry assays demonstrated that *Bm*K CT combined with TMZ significantly enhanced apoptotic activity and attenuated cell growth.

The results of the present study also demonstrated that the *Bm*K CT protein may inhibit AKT activity and increase U251 glioma cell sensitivity to TMZ. Activation of caspase-9 and caspase-3 was significantly increased in the U251 cells treated with *Bm*K CT for 96 h. In addition, GST-*Bm*K CT was revealed to increase the transcription of PTEN. Although *Bm*K CT was demonstrated to act synergistically with TMZ in inhibiting U251 glioma cell proliferation and generating the highest apoptotic rates, the use of only the U251 cell line is a limitation of the present study. The feasibility of the *Bm*K CT with TMZ combination treatment requires further study in other cell lines.

In conclusion, the results of the present study demonstrated that *Bm*K CT was able to enhance the cytotoxicity of TMZ by downregulating the levels of p-AKT. The results also suggest that *Bm*K CT combined with TMZ is a promising approach for glioma therapy.

Acknowledgements

The authors wish to thank Dr Yan Wang of Stanford University (Stanford, CA, USA) for assistance with editing. The present study was supported by the National Natural Science Foundation of China (grant no. 31400765), the Shanxi Province Science Foundation for Youths (grant no. 201601D202064), and the Scientific and Technological Innovation Programs of Higher Education Institutions in Shanxi (grant no. 2015117).

References

1. Cai J, Zhu P, Zhang C, Li Q, Wang Z, Li G, Wang G, Yang P, Li J, Han B, *et al*: Detection of ATRX and IDH1-R132H immunohistochemistry in the progression of 211 paired gliomas. Oncotarget 7: 16384-16395, 2016.
2. Goodenberger ML and Jenkins RB: Genetics of adult glioma. Cancer Genet 205: 613-621, 2012.
3. Li QJ, Cai JQ and Liu CY: Evolving molecular genetics of glioblastoma. Chin Med J (Engl) 129: 464-471, 2016.
4. Van Meir EG, Hadjipanayis CG, Norden AD, Shu HK, Wen PY and Olson JJ: Exciting new advances in neuro-oncology: The avenue to a cure for malignant glioma. CA Cancer J Clin 60: 166-193, 2010.
5. Jiang T, Mao Y, Ma W, Mao Q, You Y, Yang X, Jiang C, Kang C, Li X, Chen L, *et al*: CGCG clinical practice guidelines for the management of adult diffuse gliomas. Cancer Lett 375: 263-273, 2016.
6. Chamberlain MC: Temozolomide: Therapeutic limitations in the treatment of adult high-grade gliomas. Expert Rev Neurother 10: 1537-1544, 2010.
7. Yu Z, Xie G, Zhou G, Cheng Y, Zhang G, Yao G, Chen Y, Li Y and Zhao G: NVP-BEZ235, a novel dual PI3K-mTOR inhibitor displays anti-glioma activity and reduces chemoresistance to temozolomide in human glioma cells. Cancer Lett 367: 58-68, 2015.
8. West KA, Castillo SS and Dennis PA: Activation of the PI3K/Akt pathway and chemotherapeutic resistance. Drug Resist Updat 5: 234-248, 2002.
9. Bellacosa A, Kumar CC, Di Cristofano A and Testa JR: Activation of AKT kinases in cancer: Implications for therapeutic targeting. Adv Cancer Res 94: 29-86, 2005.
10. Huang H, Lin H, Zhang X and Li J: Resveratrol reverses temozolomide resistance by downregulation of MGMT in T98G glioblastoma cells by the NF-κB-dependent pathway. Oncol Rep 27: 2050-2056, 2012.
11. Shi F, Guo H, Zhang R, Liu H, Wu L, Wu Q, Liu J, Liu T and Zhang Q: The PI3K inhibitor GDC-0941 enhances radiosensitization and reduces chemoresistance to temozolomide in GBM cell lines. Neuroscience 346: 298-308, 2017.
12. Choi EJ, Cho BJ, Lee DJ, Hwang YH, Chun SH, Kim HH and Kim IA: Enhanced cytotoxic effect of radiation and temozolomide in malignant glioma cells: Targeting PI3K-AKT-mTOR signaling, HSP90 and histone deacetylases. BMC Cancer 14: 17, 2014.
13. Fan S, Sun Z, Jiang D, Dai C, Ma Y, Zhao Z, Liu H, Wu Y, Cao Z and Li W: BmKCT toxin inhibits glioma proliferation and tumor metastasis. Cancer Lett 291: 158-166, 2010.
14. Fu YJ, An N, Chan KG, Wu YB, Zheng SH and Liang AH: A model of BmK CT in inhibiting glioma cell migration via matrix metalloproteinase-2 from experimental and molecular dynamics simulation study. Biotechnol Lett 33: 1309-1317, 2011.
15. Fu YJ, Yin LT, Liang AH, Zhang CF, Wang W, Chai BF, Yang JY and Fan XJ: Therapeutic potential of chlorotoxin-like neurotoxin from the Chinese scorpion for human gliomas. Neurosci Lett 412: 62-67, 2007.

16. Soroceanu L, Manning TJ Jr and Sontheimer H: Modulation of glioma cell migration and invasion using Cl(-) and K(+) ion channel blockers. J Neurosci 19: 5942-5954, 1999.
17. Wang P, Ye JA, Hou CX, Zhou D and Zhan SQ: Combination of lentivirus-mediated silencing of PPM1D and temozolomide chemotherapy eradicates malignant glioma through cell apoptosis and cell cycle arrest. Oncol Rep 36: 2544-2552, 2016.
18. Batista LF, Roos WP, Kaina B and Menck CF: p53 mutant human glioma cells are sensitive to UV-C-induced apoptosis due to impaired cyclobutane pyrimidine dimer removal. Mol Cancer Res 7: 237-246, 2009.
19. Livak KJ and Schmittgen TD: Analysis of relative gene expression data using real-time quantitative PCR and the 2(-Delta Delta C(T)) method. Methods 25: 402-408, 2001.
20. Zhao L, Au JL and Wientjes MG: Comparison of methods for evaluating drug-drug interaction. Front Biosci (Elite Ed) 2: 241-249, 2010.
21. Cantley LC and Neel BG: New insights into tumor suppression: PTEN suppresses tumor formation by restraining the phosphoinositide 3-kinase/AKT pathway. Proc Natl Acad Sci USA 96: 4240-4245, 1999.
22. Sarkaria JN, Kitange GJ, James CD, Plummer R, Calvert H, Weller M and Wick W: Mechanisms of chemoresistance to alkylating agents in malignant glioma. Clin Cancer Res 14: 2900-2908, 2008.
23. Gallia GL, Tyler BM, Hann CL, Siu IM, Giranda VL, Vescovi AL, Brem H and Riggins GJ: Inhibition of Akt inhibits growth of glioblastoma and glioblastoma stem-like cells. Mol Cancer Ther 8: 386-393, 2009.